Point-Surface-Origin Macropitting Caused by Geometric Stress Concentration

R.L. Errichello, C. Hewette and R. Eckert

Management Summary

Point-surface-origin (PSO) macropitting occurs at sites of geometric stress concentration (GSC) such as discontinuities in the gear tooth profile caused by micropitting, cusps at the intersection of the involute profile and the trochoidal root fillet, and at edges of prior tooth damage, such as tip-to-root interference. When the profile modifications in the form of tip relief, root relief, or both, are inadequate to compensate for deflection of the gear mesh, tip-to-root interference occurs. The interference can occur at either end of the path of contact, but the damage is usually more severe near the start-of-active-profile (SAP) of the driving gear.

An FZG-C gear set (with no profile modifications) was tested at load stage 9, and three pinion teeth failed by PSO macropitting. It is shown that the root cause of the PSO macropitting was GSC created by tip-to-root interference.

Introduction

Stewart Way (Ref. 1) first described what later became known as point-surface-origin macropitting. The macropits are relatively shallow, but large in area. The fatigue crack grows from a surface origin in a fan-shaped manner until thin flakes of material break out and form a triangular crater. The arrowhead-shaped crater points opposite the direction of rolling (direction of load approach). Crack propagation can extend over large portions of a gear tooth. Way (Ref. 1) also proposed a theory of hydraulic-pressure-propagation to explain the growth of PSO macropits. Lubricant viscosity is an important parameter influencing PSO macropitting, and it has been shown (Ref. 2) that low-viscosity lubricants promote PSO macropitting by hydraulic-pressure-propagation. PSO macropitting results from the combination of low-viscosity lubricant, low specific-film thickness and tangential shear stresses from sliding (Ref. 2). PSO macropitting can originate from surface flaws such as:

- Tip-to-root interference
- Debris dent
- Handling nick
- Edge of macropitting
- Edge of micropitting
- Surface flaws from manufacturing
- Surface non-metallic inclusion
- Surface carbide
- Corrosion pit

This paper discusses PSO macropitting originating from tip-to-root interference. If involute gear teeth were perfectly rigid and without manufacturing errors, they would begin contact at the ideal start-of-active-profile (SAP) point and end contact at the ideal end-of-active-profile (EAP) point.

However, real gears are not rigid, and even without manufacturing errors, tooth deflection causes the teeth to start contact earlier than the ideal SAP, and end contact later than the ideal EAP. In the areas of extended contact at the ends of the path-of-contact, a gear tooth is loaded on its tip corner (intersection between the tooth flank and tooth top-land) and the contact stresses are very high because of geometric stress concentration (GSC). Therefore, to avoid corner contact and the associated high-contact stresses, it is common practice to design gear teeth with tip relief that is sufficient to compensate for tooth deflection and manufacturing errors. However, FZG-C test (spur) gears (FZG-C) are manufactured accurately but without tip relief. Consequently, they inevitably have corner contact when they are tested at high loads. FZG-C gears are discussed in this paper because they demonstrate the consequences of inadequate tip relief.

Objective

This paper demonstrates how gears without tip relief suffer tip-to-root interference that causes GSC and PSO macropitting.

Corner contact. Figure 1 shows the path-of-contact for FZG-C gears that was calculated with *KISSsoft* software (Ref. 3). It shows corner contact occurs when accompanied by early contact between the gear tip and the pinion involute at point A', and continues along the gear tip circle to point A on the line of action. The path-of-contact between points A' and A is non-conjugate and is known by many names, including:

- Tip-to-root interference
- Corner contact
- Contact outside the normal path of contact
- Early contact
- Edge contact
- Extended contact
- Non-conjugate action
- Premature contact
- Prolonged contact
- Top contact
- Tooth interference

Mechanism of tip-to-root interference. Figure 2 shows how the gear tip corner approaches the pinion involute along a trochoidal path that intersects the pinion involute at a point above the usual pinion SAP. Contact between the gear corner and the pinion involute results in very high Hertzian stress—especially if the gear has sharp corners at the tips of its teeth. The high stress and scraping action of the gear corner undercut the pinion involute by removing the material (shown shaded in Fig. 2) and plowing material toward the pinion root. The intersection between the undercut and involute forms a cusp on the pinion flank at point A'. In this paper, damage caused by corner contact will be called tip-to-root interference.

Contact on pinion cusp. Corner contact undercuts the pinion involute and removes the usual SAP (point A) and delays the contact between the pinion and gear until they contact at point A″ on the line of action as shown in Figure 3. The edge contact that occurs on the pinion cusp causes GSC, as shown by the local maximum Hertzian stress illus-
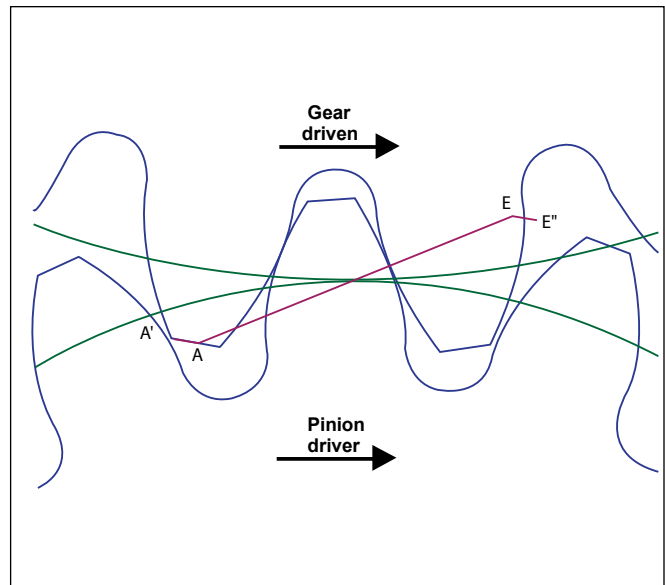
continued

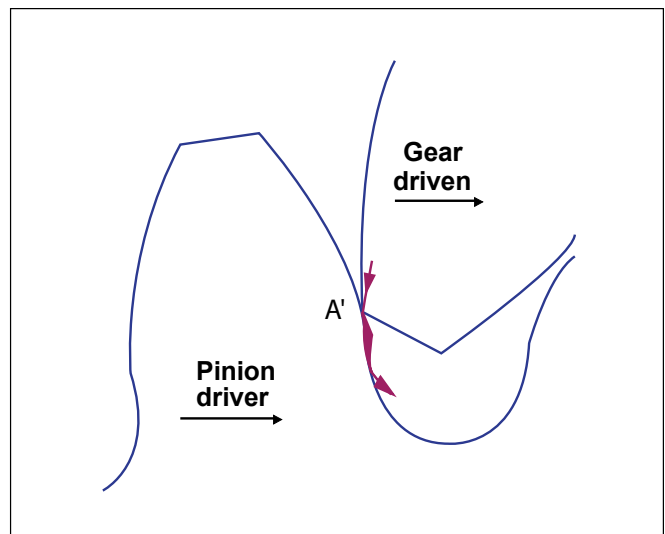Figure 1—Gear tip approaching pinion involute.

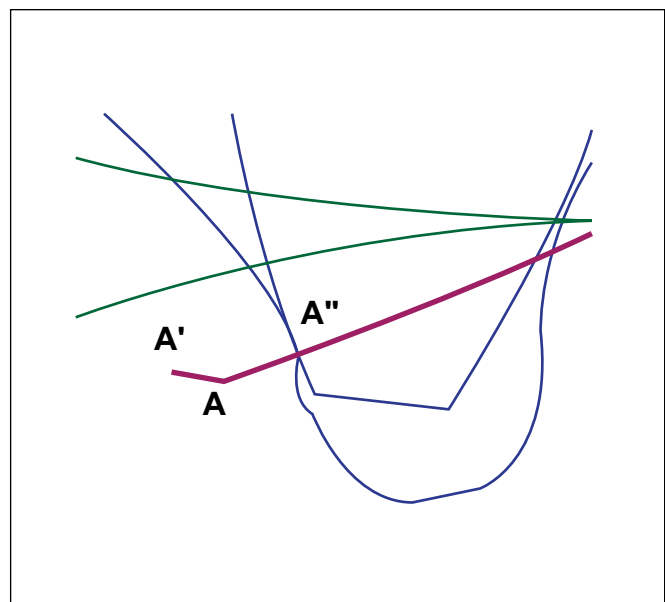Figure 2—Mechanism of tip-to-root interference.
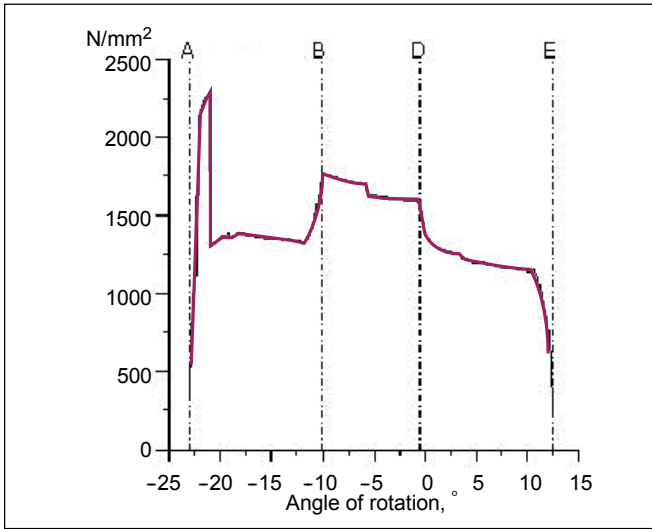

Figure 3—Contact on the pinion cusp.

Figure 4—Local maximum Hertzian stress at pinion cusp.

Table 1—Lubricant Properties	
Type	Mineral oil including 325 Neutral and 650 Neutral Group I
Additives	VI-improver, pour point depressant, mild S-P antiscuff
Viscosity at 40°C	157.2 cSt
Viscosity at 100°C	18.3 cSt

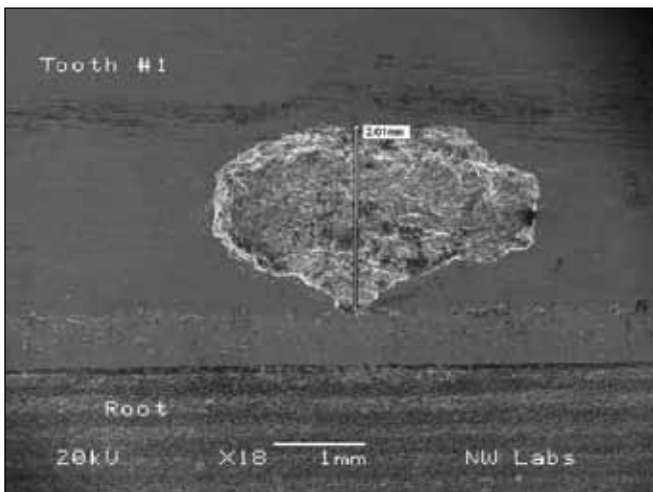Figure 5—Damage caused by tip-to-root interference on pinion.

Figure 6—Enlarged view of PSO macropit on pinion.

trated in Figure 4.

FZG-C test gears. An FZG-C gear set was tested at load stage 9 in accordance with the FZG pitting test PT C/9/90 procedure (Ref. 4), except the oil temperature was set to 120°C. Table 1 gives the lubricant properties. The lubricant prevented adhesive and abrasive wear. However, after only
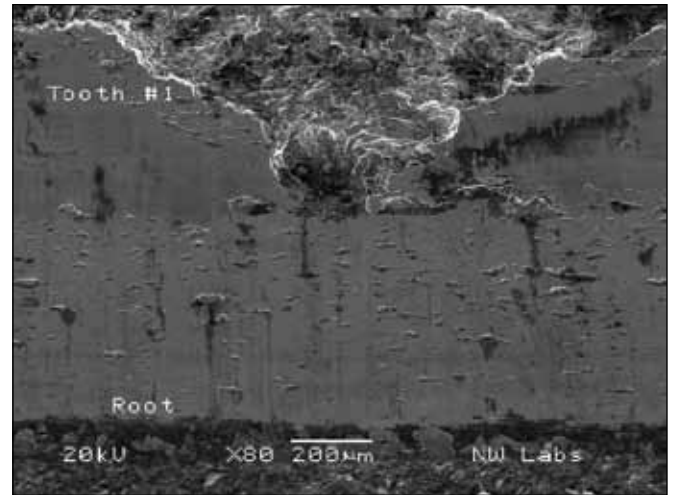

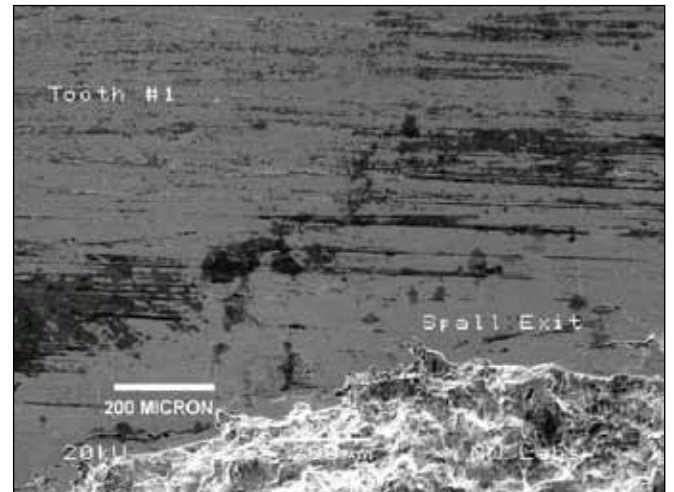Figure 7—Enlarged view at entrance of PSO macropit on pinion.

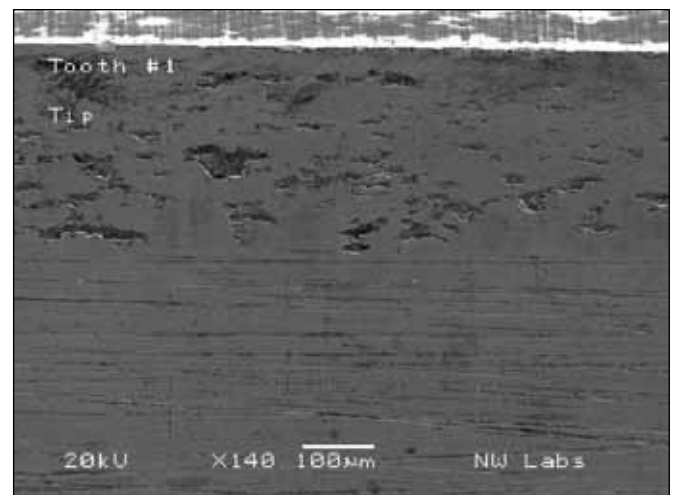Figure 8—Enlarged view at exit of PSO macropit on pinion.

Figure 9—Enlarged view at tip of tooth 1 on pinion.

60 hours the test had to be stopped because macropitting occurred on teeth 1, 9 and 15.

Damage caused by tip-to-root interference. Figure 5 shows tooth number 1 of the FZG-C pinion with damage caused by tip-to-root interference. To the unaided eye, the damage might appear as a polished line along the SAP, and it is often referred to as a "line of hard contact." However, as will be shown, the damage in this example consists of plastic deformation, micropitting and PSO macropitting. In more severe cases the damage can include material transfer resulting from scuffing.

PSO macropitting. Figure 6 is an enlarged view (scanning electron image) of Figure 5 showing the largest PSO macropit—about 2 x 3.5 mm. Figure 7 is an enlarged view at the entrance of the PSO macropit, which initiated at the upper edge of the tip-to-root damage and corresponds to the cusp at point A' (Fig. 2). Below the cusp, the tip-to-root damage produced a 0.5 mm high band of plastically deformed material and a dense field of micropitting. All pinion teeth had similar tip-to-root damage, but in the short run time of 60 hours only three teeth developed relatively large PSO macropits that—in each case—initiated at the cusp.

Figures 5, 6 and 7 show there are many other PSO macropits that have initiated at the cusp but have not yet grown significantly. Figure 8 is an enlarged view at the exit of the PSO macropit. Original grind marks can be seen above the macropit, proving that there was no significant adhesive or abrasive wear on the pinion flanks.

Figure 9 is an enlarged view at the tip of tooth number 1. It shows micropitting caused by tip-to-root interference between the pinion tip and the gear root. Original grind marks are evident below the micropitting, proving that there was no significant adhesive or abrasive wear on the pinion flanks.

Figure 10 shows a PSO macropit that occurred on tooth 15 that measures about 1.8 x 2.8 mm. Two other macropits can be seen initiating at the cusp (upper edge of the tip-to-root damage).

Figure 11 shows a PSO macropit that occurred on tooth 9 that measures about 1.5 x 1.5 mm. At least two other macropits can be seen initiating at the cusp (upper edge of the tip-to-root damage). The micropitting within the band of tip-to-root interference is not as obvious in this light micrograph as it is in the other scanning electron images (Figs. 6, 7 and 10). However, the abrasion within the tip-to-root interference and the original grind marks on the flank are more obvious.

Gear tooth sliding. Figure 12 shows the directions of the rolling (R) and sliding (S) velocities on the driving and driven gear teeth. Contact on the driving tooth starts near the root of the tooth, rolls up the tooth and ends at the tooth tip. Sliding is away from the driving gear pitch line. Contact on the driven tooth starts at the tooth tip, rolls down the tooth and ends near the tooth root. Sliding is towards the driven gear pitch line.

Hertzian fatigue cracks—both macropitting and micropitting—that start at the gear tooth surface grow at a shallow angle to the surface, opposite that of the slide directions. Consequently, as shown in Figure 12, the cracks converge near the pitch line of the driver and diverge near the pitch line of the driven gear.

Hydraulic-pressure-propagation. Gear teeth dedenda have negative sliding (i.e., direction of rolling velocity is opposite sliding velocity). Negative sliding is significant because it promotes Hertzian fatigue by allowing oil to enter surface cracks where it accelerates crack growth by the hydraulic-pressure-propagation mechanism first proposed by
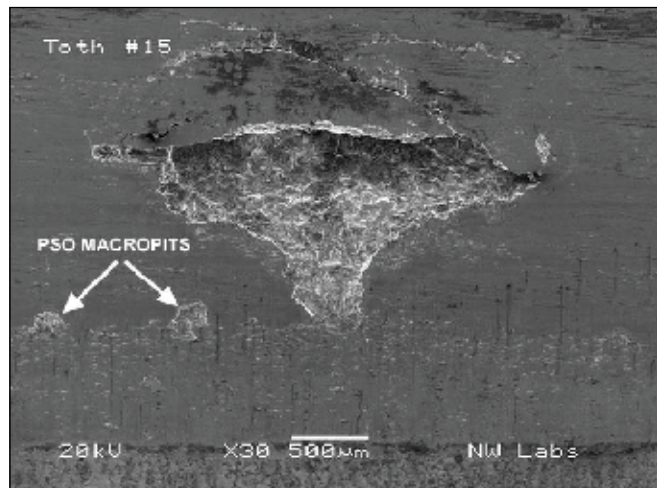
continued

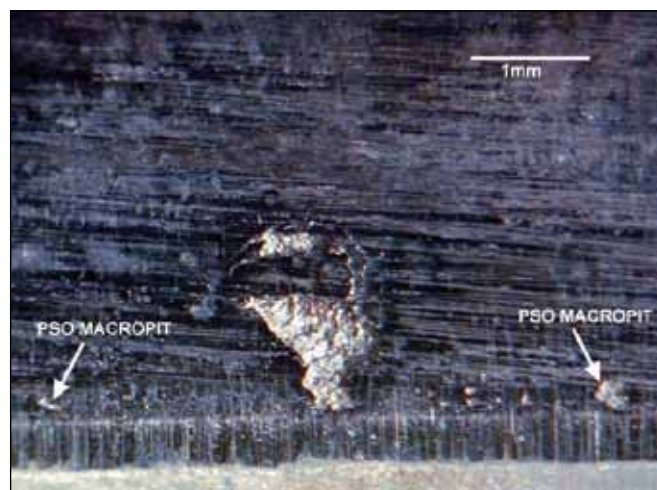**Figure 10—PSO macropit on tooth 15 on pinion.**

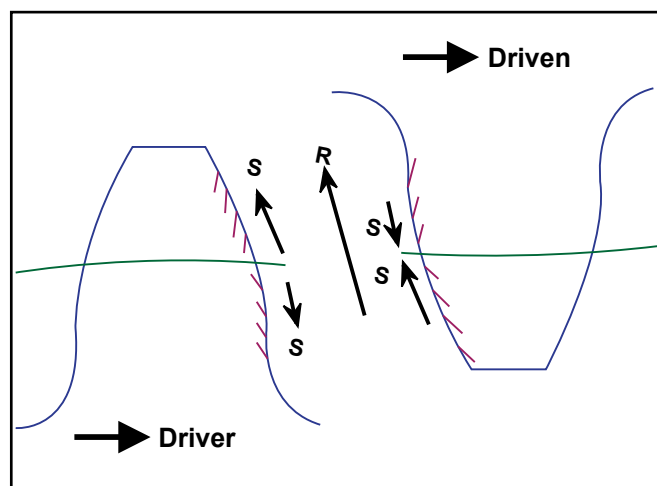**Figure 11—PSO macropit on tooth 9 on pinion.**

Figure 12—Rolling (R) and sliding (S) directions.

Way (Ref. 1) and verified many times by experiments such as Littmann's (Ref. 2).

Hertzian stress resulting from GSC. GSC associated with contact on the pinion cusp creates a Hertzian stress that is theoretically infinite, but is actually limited to the yield strength of the pinion material. Therefore, the cusp plastically deforms and the GSC is reduced. However, carburized gears have high yield strength, and even though subsequent cyclic stresses are elastic, the stresses are generally high enough to initiate macropitting. Li, et al., (Ref. 5) tested FZG PT-C macropitting gears and found that in all cases PSO macropits initiated at the cusp of the tip-to-root damage. Furthermore, they measured the radius of the cusp on several damaged teeth of a pinion and found it averaged 1.54 mm. They assumed the mating gear radius-of-curvature at point A″ was 26.76 mm and calculated the relative radius-of-curvature was 1.46 mm. For unworn teeth they calculated a relative radius-of-curvature of 6.26 mm. According to Hertzian theory, the difference in relative radius-of-curvature doubles the Hertzian maximum shear stress, but reduces its depth to only half as deep. Consequently, the stress increase resulting from GSC is very significant and it explains why PSO macropits initiate at the cusp.

Jao, et al, (Ref. 6) tested FZG PT-C macropitting gears and FZG GF-C micropitting gears that are identical in all respects except that PT-C gears have a tooth-surface-roughness of Ra = 0.3 μm, whereas GF-C gears have tooth-surface-roughness of Ra = 0.5 μm. With PT-C gears, PSO macropits initiate at the cusp formed by tip-to-root interference. In contrast, the GF-C gears form a band of micropitting at the SAP similar to PT-C gears, but in this case it continues to spread toward the pitch line until forming a wide band of severe micropitting. PSO macropits initiate at the top of the micropitting band because of GSC caused by the step in the tooth profile at the upper edge of the micropitting crater; this macropitting occurs later than with the PT-C gears. The authors concluded that the failure mechanism is different for GF-C gears because their rougher surfaces cause more severe micropitting that removes the cusp at the SAP and thereby prolongs macropitting life.

Conclusions
- The root cause of PSO macropitting is the GSC caused by tip-to-root interference, or GSC caused by edge discontinuities such as the edge of a band of micropitting.
- Tip-to-root interference is caused by corner contact that occurs in gears without adequate tip relief.
- Tip-to-root interference undercuts the involute profile and creates a cusp on the active flank that acts as a point of GSC.
- With FZG PT-C gears, PSO macropits initiate at the cusp formed by tip-to-root interference.
- With FZG GF-C gears, their rougher surfaces cause more severe micropitting that removes the cusp at the SAP—and thereby prolongs macropitting life—

Rainer Eckert's *academic background includes a bachelor of science and engineering degree in 1983 from Technical University of Berlin, where he was also named "Best Graduate of Engineering" in his class; and a master of science and engineering in materials science from the University of Pennsylvania in 1985. He has since 1986 been employed as a forensic engineer and director of the metallurgical services department at Northwest Laboratories in Seattle, WA. Previously, Eckert has worked as both research and consulting assistant at various stops, including the University of Pennsylvania and the Welding Institute of Berlin, and for four years (1979–1983) was a mechanic at his own auto repair shop. Eckert is a member of the American Institute of Metallurgical Engineers, the American Society of Metals and the German Society of Engineers.*

Robert Errichello *heads his own gear consulting firm— GEARTECH—and is a founder of GEARTECH Software, Inc. He is a registered professional engineer and a graduate of the University of California at Berkeley. He holds B.S. and M.S. degrees in mechanical engineering and a master of engineering degree in structural dynamics. Errichello has over 34 years of industrial experience and has worked for several gear companies. He has been a consultant to the gear industry for the past 19 years; has taught courses in material science, fracture mechanics, vibration and machine design at San Francisco State University and the University of California at Berkeley; and is a member of ASM International,*

STLE, ASME Power Transmission and Gearing Committee, AGMA Gear Rating Committee and the AGMA/AWEA Wind Turbine Committee. Errichello has published over 40 articles on design, analysis and the application of gears and is the author of three widely used computer programs for the design and analysis of gears. He is a technical editor for **Gear Technology** *magazine and STLE Tribology Transactions and has presented numerous seminars on design, analysis, lubrication and failure analysis of gears. Errichello is a recipient of the AGMA TDEC Award and the STLE Wilbur Deutch Memorial Award.*

Chip Hewette *is a lubricant formulator with Afton Chemical Corporation, a worldwide supplier of lubricant additives. His main efforts are in improving vehicle fuel efficiency and reducing noise, vibration and harshness (NVH) in systems such as limited slip differentials. Hewette's background is primarily mechanical engineering, concentrating on product design. His experiences include the design of EGR valves, position sensors and HVAC compressors. Other endeavors have included product warranty management, manufacturing quality and process improvement consulting. He received his B.E. in mechanical engineering from Vanderbilt University in 1983, and is a licensed professional engineer. He holds U.S. patents in a variety of fields. Hewette lives in Henrico, VA with his wife and two daughters.*

until PSO macropitting occurs near the pitch line due to GSC caused by the step in the tooth profile at the upper edge of the micropitting crater.

- PSO macropitting occurs from the combination of low-viscosity lubricant, low specific-film thickness and tangential shear stresses from sliding.
- Negative sliding promotes rapid growth of PSO macropitting by the hydraulic-pressure-propagation mechanism. ⚙

References
1. Way, S. "Pitting Due to Rolling Contact," ASME Trans., *J. Appl. Mech.*, Vol. 57, pp. A49-A114, 1935.
2. Littmann, W.E. "The Mechanism of Contact Fatigue—An Interdisciplinary Approach to the Lubrication of Concentrated Contacts," SP–237, NASA, pp. 309–377, 1970.
3. 09FTM06, Kissling, U. "Dependency of the Peak-to-Peak Transmission Error on the Type of Profile Correction and the Transverse Contact Ratio of the Gear Pair," AGMA, 2009.
4. FVA Information Sheet No. 2/IV, "Pitting Test," Forschung svereinigung Antriebstechnik E.V. July, 1997.
5. SAE Paper 2003–01–3233, Li, S. et al. "Investigation of Pitting Mechanism in the FZG Pitting Test," 2003.
6. 04FTM04, Jao, T.C. et al. "Influence of Surface Roughness on Gear Pitting Behavior," AGMA, 2004.

Appendix A
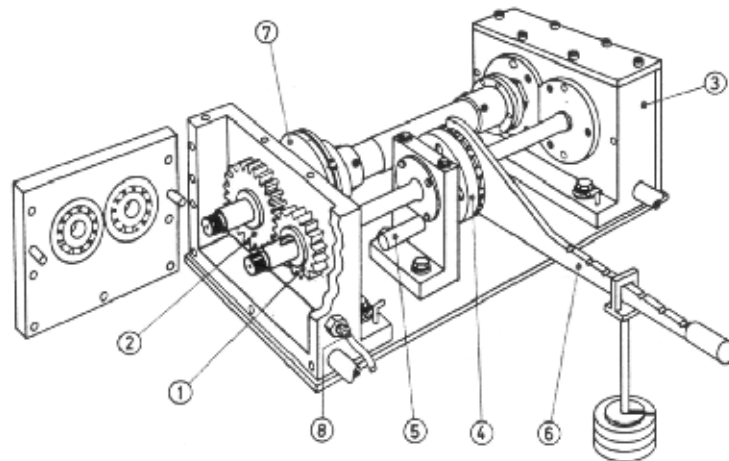
1 pinion
2 gear wheel
3 drive gears
4 load clutch
5 locking pin
6 lever arm with weight pieces
7 torque measuring clutch
8 temperature sensor

FZG test machine

Table A1—Data for Test Gears				
Item	Symbol	Unit	FZG PT-C	FZG GF-C
Center distance	a	mm	91.5	
Number of pinion teeth	z_1	---	16	
Number of gear teeth	z_2	---	24	
Normal module	m_n	mm	4.5	
Normal pressure angle	α_n	deg	20	
Helix angle	β	deg	0	
Face width	b	mm	14	
Pinion profile shift coefficient	x_1	---	0.1817	
Gear profile shift coefficient	x_2	---	0,1715	
Pinion tip diameter	d_{a1}	mm	82.46	
Gear tip diameter	d_{a2}	mm	118.36	
Material alloy	---	---	16MnCr5	
Heat treatment	---	---	Carburized	
Flank surface roughness	R_a	μm	0.3 ± 0.1	0.5 ± 0.1
Pitchline velocity	v_t	m/s	8.3	